

PAPER • OPEN ACCESS

Kinetic contributions rule diffusion of mass in the liquid ternary eutectic E1 Ag–Al–Cu alloy

To cite this article: M Engelhardt et al 2025 J. Phys.: Condens. Matter 37 385401

View the article online for updates and enhancements.

You may also like

- The quality assessment of radial and tangential neutron radiography beamlines of TRR
- of TRR M.H. Choopan Dastjerdi, A. Movafeghi, H. Khalafi et al.
- Advances in neutron radiography and tomography
 M Strobl, I Manke, N Kardjilov et al.
- Kinematics, Kinetic Temperatures, and <u>Column Densities of NH₃ in the Orion Hot</u> <u>Core</u>
- Core
 T. L. Wilson, R. A. Gaume, P. Gensheimer et al.

J. Phys.: Condens. Matter 37 (2025) 385401 (11pp)

https://doi.org/10.1088/1361-648X/ae0259

Kinetic contributions rule diffusion of mass in the liquid ternary eutectic E1 Ag-Al-Cu alloy

M Engelhardt, F Karglo, E Sondermann* and A Meyer

Institut für Materialphysik im Weltraum, Deutsches Zentrum für Luft- und Raumfahrt (DLR), 51170 Köln, Germany

E-mail: elke.sondermann@dlr.de

Received 26 March 2025, revised 1 August 2025 Accepted for publication 2 September 2025 Published 19 September 2025



Abstract

In ternary alloy systems, the mass diffusion of one component can be influenced by interactions with other constituents caused by their chemical concentration gradients. The diffusion coefficients of the ternary system around its eutectic composition (Al_{69.1}Ag_{18.1}Cu_{12.8} [at%]) were measured in the liquid state. The *ex-situ* shear cell (SC) method combined with *in-situ* neutron radiography (NR) measurements of diffusion couples processed in a long-capillary, as a benchmark experiment, provides significantly enhanced accuracy compared to the long capillary method with post-mortem analysis. Based on these measurements, it is shown that no uphill diffusion occurs. This result is supported by the obtained diffusion matrix. The diffusion coefficients obtained from the SC and NR experiments coincide within their margins of error of 10%. Complementary quasi-elastic neutron scattering measurements of self-diffusion show that interdiffusion and self-diffusion agree in the eutectic Al–Ag–Cu melt, revealing the dominant influence of kinetic contributions to interdiffusion.

Keywords: diffusion, ternary alloy, neutron scattering

1. Introduction

The mechanical and physical properties of materials are determined by their microstructure formation. The first important step is the solidification of the molten material. A profound understanding of the processes at the solid—liquid interface between different phases during solidification, as well as detailed knowledge of the melt dynamics,

Original Content from this work may be used under the terms of the Creative Commons Attribution 4.0 licence. Any further distribution of this work must maintain attribution to the author(s) and the title of the work, journal citation and DOI.

are essential for modeling solidification and crystal growth processes [1, 2].

In multicomponent materials, using a single diffusion coefficient is generally not sufficient to describe crystal growth; knowledge of multicomponent diffusion is required [3]. In a ternary material, diffusion is characterized by three self-diffusion coefficients and a 2×2 matrix for chemical diffusion [4]. The diagonal elements of this matrix give the main diffusion coefficients, and the off-diagonal elements give the cross diffusion coefficients, which describe the mass transport of one component caused by a concentration gradient of another component [5, 6]. Measurements of chemical diffusion in an organic ternary liquid showed that the off-diagonal elements can be of the same order as the diagonal ones [7]. Significant cross-diffusion coefficients are also observed in solid alloys [8–10].

^{*} Author to whom any correspondence should be addressed.

Despite their importance, diffusion measurements for ternary metallic melts are extremely scarce [11]. For some alloys, phenomenological models have been employed to derive the ternary diffusion coefficients from those of the corresponding binary alloys [2, 12, 13]. However, measurements are essential in order to establish benchmark coefficients that can be used to test the reliability of the predicted values [14].

Measuring diffusion coefficients in liquid alloys presents a number of experimental challenges. The most significant of these are the flow effects that occur during the melting of the diffusion couple, buoyancy-driven convection during diffusion annealing, the formation of shrinkage, and mass transport due to microstructure formation during solidification [15].

Traditionally, diffusion coefficients are measured by determining concentration profiles of different elements in a solidified sample. An important technique in this respect is the long-capillary technique [16, 17]. In this technique, the spatial distribution of a tracer or the spatial dependence of composition along a thin rod-shaped sample is determined after a full heating, annealing, and cooling cycle. This technique has proven highly successful for solids. However, in liquids, the accuracy of the data used to determine the diffusion coefficient is negatively affected by convection during annealing and by changes in concentration or isotope distribution during melting and solidification. Such derived diffusion data show a large scatter [18–20].

The development of new measurement methods allowed the measurement of reproducible diffusion coefficients [21]. For binary systems, accurate diffusion coefficients can be obtained by monitoring the long capillary (LC) *in-situ* using x-ray or NR [22, 23]. However, to determine accurate diffusion coefficients for alloys with insufficient or no contrast, the so-called shear cell (SC) method has to be applied, whereby individually solidified slices of the diffusion couple are analyzed post-experiment [11, 24, 25].

We use different measurement methods to investigate how kinetics define the mass transport, and to determine the influence of thermodynamic driving forces on the interdiffusion coefficient. The relationship between self-diffusion and interdiffusion was studied in various binary liquid alloys [26–30] with the conclusion that in melts with a strong thermodynamic tendency to mix, such as Ni-Zr or Al-Ni, a dominant kinetic contribution to interdiffusion is observed [27, 28, 31]. The relationship between self-diffusion and interdiffusion in multicomponent mixtures can be described by the Darken equation [32, 33]. This equation provides an approximation for interdiffusion coefficients by neglecting cross-correlation terms in the autocorrelation functions [26]. Molecular dynamics simulations have shown that, for ternary mixtures containing only light weighted components, the Darken approximation yields interdiffusion coefficients within 10%-20% of the complete formulation. However, for ternary mixtures where the mass of the components is highly asymmetric the Darken equation can be off by a factor of two [34].

We present benchmark diffusion data for the eutectic Al_{69.1}Ag_{18.1}Cu_{12.8} [at%], which has a large thermodynamic factor [35], and therefore a thermodynamic influence on

interdiffusion can be expected. Furthermore, the low melting temperature of approximately 770 K facilitates experimentation and reduces the risk of temperature gradients across the sample, which could cause Marangoni convection [36–38]. The microstructure of eutectic Ag–Al–Cu has been investigated using 3D synchrotron imaging and other techniques [39, 40].

2. Experimental techniques

2.1. Sample preparation

The capillary samples were produced by arc melting in a high-purity Ar atmosphere (6 N argon + Oxisorb) using Al (99.99%, Chempur), Cu (99.999%, Chempur), and Ag (99.9%, Chempur). The samples were melted three times for homogenization and then poured by suction casting into a water-cooled copper mould, resulting in cylindrical rods with a diameter of 1.45 mm that were cut to length. Using x-radiography, homogeneous samples without shrinkage holes were selected. The composition of the sample was verified by weighing the raw materials, as well as the samples, after each step of the synthesis, and the application of energy dispersive x-ray spectroscopy (INCA Oxford) with a LEO 1530 VP scanning electron microscope. No evaporation or other loss of sample material occured.

2.2. Chemical diffusion measurements

To determine of the chemical diffusion coefficients in the Al_{69.1}Ag_{18.1}Cu_{12.8} ternary system, complementary measurement methods were employed, including an enhancement of the traditional LC method, the SC method, and NR.

In the traditional LC method, thin cylindrical samples with slightly different compositions, typically measuring 1–1.5 mm in diameter and 10-40 mm in length, are brought into contact with each other. Typically, a sample pair is inserted into a capillary made of graphite, for example, and subsequently heated to the diffusion temperature above the melting point. It is then kept there for a defined period of time before being solidified. Stable density layering [41], a relatively thin capillary [36] and a constant temperature profile along the sample [42] are crucial for LC experiments conducted under gravity conditions, as they minimize the occurrence and influence of convection in the sample. Using sample pairs with different compositions of the same alloy enables the determination of the interdiffusion coefficient through the analysis of the concentration profile during (in-situ) and after (ex-situ) experiment conduction [43]. In a standard LC experiment, the full experiment cycle is conducted from melting of the sample, diffusion annealing at a constant temperature, and finally solidifying it. The LC experiment setup used here consists of a modified tube furnace that can be moved downwards in order to surround the crucible, and ensuring fast heating of the samples and a homogeneous temperature distribution during annealing. The tube furnace can then be moved upwards by a hoist to enable fast cooling. Thermocouples are used to monitor the temperature of the sample and its surroundings, and a homogeneous temperature distribution has been verified. The entire setup is placed on a granite plate with air cushioning to prevent the sample from vibrating. The crucible containing the sample is inside an evacuated fused quartz tube. The crucible itself consists of a graphite tube which is placed inside a slightly larger graphite tube to provide mechanical stability and temperature homogenization. Graphite felt is used as a spring to press down on a graphite piston, compensating for the volume change of the sample during heating and melting. The sample, consisting of a diffusion pair, has a diameter of 1.5 mm and is between 40 and 50 mm long. This enables annealing times between 45 and 60 min. This comparatively long annealing time ensures that the influence of diffusion during time needed for melting and solidification of the samples is minimized.

A substantial disadvantage of *ex-situ* analysis is the lack of process control. Disturbing effects such as bubble formation, sedimentation, and free surfaces between the sample and the container wall are difficult to detect. Therefore, a correct interpretation of the diffusion profile and extraction of an accurate diffusion coefficient is impeded. Furthermore, convective flow arising during the melting and solidification of the samples alters the concentration profile, thereby introducing an additional source of error. Improving the LC method by combining it with x-ray radiography (XRR) helped to overcome some of the aforementioned limitations [22, 44]. However, this method is limited to alloys with sufficient x-ray contrast. The often complementary cross sections of XRR and NR allow access to some systems via NR. As in XRR, NR involves measuring the attenuation of the beam along the sample and converting the obtained gray-scale distribution into concentrations. A Gaussian error function is fitted to the concentration profile. The diffusion coefficient can then be obtained from the fitting parameters at different times during the diffusion process. Further details of the NR setup can be found here [23].

The SC method is an improvement on the traditional ex-situ LC method. It minimizes disturbance to the liquid sample during melting and solidification by separating the diffusion samples. The graphite SC [25] used in this study is an enhancement on the SC version employed on the FOTON satellite mission [45], facilitating the processing of up to six samples in one experimental cycle at temperatures of up to 1600 °C. The SCs are comprise 28 graphite discs, each with a diameter of 30 mm, a thickness of 3 mm, and 6 bores with a diameter of 1.5 mm, evenly distributed on a circle with a radius of 8.5 mm. Placing all discs on top of each other with the bores aligned, results in six long capillaries for six sample pairs. Rotating individual discs separates the sample segments, allowing them to melt and homogenize independently. The number of discs limits the spatial resolution of the subsequent analysis. In the initial configuration of the SC, only the disc at the sample pair interface is rotated, which prevents shear convection between the other segments at the start of the actual experiment. At the beginning of the diffusion process, once the diffusion temperature T_{Diff} has been reached, the discs are perfectly aligned, bringing the sample pairs into contact. This rotation is initiated only after the heating phase has been completed and the SC temperature has been homogenized, in order to diminish any potential turbulence in the melt that might have emerged during the heating process. This configuration is maintained for a predefined process duration. At the end of the diffusion experiment, all segments of the SC are separated, thereby freezing the current concentration profile of the liquid column and decoupling it from the cooling period and solidification process. The errors occurring during the solidification phase are therefore contained within the individual segments. However, they do not impact the diffusion profile, since the average composition of each segment is measured by chemical analysis.

To ensure a comparable behavior between similar sample systems using different measurement methods and to exclude reactions with the material surrounding the samples, identical graphite raw material was used for all measurement methods. Only for the NR experiments, Al_2O_3 was used due to the neutron scattering in graphite [23]. The diffusion temperatures were adjusted to a range of 983–993 K. For the LC methods, this temperature deviated by up to \pm 3 K, whereas for the SC method, it varied by less than \pm 1 K. The temperature of 983 K was chosen to make sure that the diffusion pairs, which due to their composition have a higher melting point than the eutectic composition, were fully liquid. The vacuum for all interdiffusion experiments was of the order of 10^{-3} mbar.

2.3. Self-diffusion measurement

Quasi-elastic neutron scattering (QENS) was used to measure the self-diffusion in liquid Al_{69.1}Ag_{18.1}Cu_{12.8} at various temperatures. For elements that contribute to the inelastic scattering of neutrons, the scattering signal at small wave numbers q is dominated by the incoherent contributions. The selfdiffusion coefficient can be obtained from the resulting intermediate scattering function. This technique probes the dynamics on atomic length and picosecond timescales and is unaffected by convective flow [46, 47]. Measurements were carried out at the neutron time-of-flight spectrometer TOFTOF [48] at the research neutron source Heinz Maier-Leibnitz (FRM II) in Garching. The sample material was placed in thin-walled Al₂O₃ containers providing a hollow cylindrical sample geometry of 22 mm in diameter and a thickness of 1.2 mm. The incident neutron wavelength of $\lambda = 5.4 \text{ Å}$ yielded an energy resolution of $\delta E \simeq 85 \,\mu\text{eV}$ (FWHM) and an accessible wave number range at zero energy transfer of $q = 0.4 - 2.0 \text{ Å}^{-1}$.

3. Results and discussion

In the analysis of diffusion profiles, a quasi-binary sample is assumed for a ternary alloy, where one component has a constant concentration throughout the sample. This component does not interact with the others, has no influence on their diffusion processes, and remains constant after the experiment. The two varying components can then be treated as a binary system, and the analysis can be conducted as for any binary system. However, if the concentrations of all three components change, the system must be treated as a true ternary system, and the diffusion coefficients must be derived using a diffusion matrix.

Table 1. Sample composition of the three sample pairs with one constant constituent concentration each. These ternary alloys can be considered quasi-binary.

Sample pair	Sample composition in at%
#1	$Al_{63.6}Cu_{18.8}Ag_{17.6}/Al_{73.6}Cu_{8.8}Ag_{17.6}$
#2	$Al_{68.6}Cu_{18.8}Ag_{12.6}/Al_{68.6}Cu_{8.8}Ag_{22.6}$
#3	$Al_{73.6}Cu_{13.8}Ag_{12.6}/Al_{63.6}Cu_{13.8}Ag_{22.6}$

Table 2. Sample composition of the three sample pairs with three varying constituent concentrations each. These ternary alloys cannot be considered quasi-binary.

Sample pair	Sample composition in at%	
#4 #5	$Al_{71.5}Cu_{8.0}Ag_{20.5}/Al_{65.7}Cu_{19.6}Ag_{14.7}$	
#6	$\begin{array}{l} Al_{65.7}Cu_{10.9}Ag_{23.4}/Al_{63.6}Cu_{16.7}Ag_{11.8} \\ Al_{62.8}Cu_{16.7}Ag_{20.5}/Al_{74.4}Cu_{10.9}Ag_{14.7} \end{array}$	

In solids, it may be possible to obtain diffusion coefficients in multicomponent systems from a single diffusion profile [49]. For liquids, several diffusion pairs are needed. In this study, six Ag–Al–Cu sample pairs close to the ternary eutectic Al_{69.1}Ag_{18.1}Cu_{12.8} [at%] were investigated. For three of the sample pairs, the concentration of one alloy constituent was kept constant (see table 1). For the other three ternary sample pairs, all component concentrations varied (see table 2). Different, complementary measurement methods were employed and the individual results were compared.

3.1. Quasi-binary analysis

At the beginning of this study, approximately 50 experiments were conducted using three AlCuAg sample pairs close to the ternary eutectic Al_{69.1}Ag_{18.1}Cu_{12.8} [at%] where the concentration of one alloy constituent was kept constant in each sample pair (see table 1). All three sample pairs were examined with the *ex-situ* LC method and with the SC technique. Additionally, sample pair #3 was investigated using the NR method [23].

The diffusion coefficients of the quasi-binary sample pairs are referred to as $D_{A/B}^*$ where the coefficients A and B represent the components of the quasi-binary alloy whose concentration profiles change by diffusion during the experiment, while the concentration of the third component remains constant.

The diffusion data of these alloys, derived from quasibinary post-mortem analysis of the *ex-situ* LC experiments, are shown in figure 1 and listed in table A1. Experiments with subsequently proven errors were not taken into account. Proven sources of error included graphite blockades at the interface between the two samples, caused by the installation, free surfaces and the leakage of melt through ruptures or through the sample capillary seal.

For all three sample pairs, the mean diffusion coefficient was determined to be approximately $D_{A/B}^* = 6.3 \cdot 10^{-9} \text{m}^{-2} \, \text{s}^{-1}$. The individual values scatter between $3.0 \cdot 10^{-9} \text{m}^{-2} \, \text{s}^{-1}$ and $9.7 \cdot 10^{-9} \text{m}^{-2} \, \text{s}^{-1}$, being a

factor of more than three. A uniform error range is plotted around the average value and can be considered the error for the *ex-situ* LC data. This large error is mainly caused by the missing process control during experiment conduction. Melting, and particularly solidification, of the samples introduces additional systematic sources of error into the analysis of a full process cycle in the LC, since both processes can significantly influence the concentration profile. In summary, even with a large number of similar experiments neither the statistical mean value nor the lowest diffusion coefficient allow a conclusion concerning the real diffusion coefficient. Therefore, *in-situ* process control or alternative measurement methods, such as the SC method, are preferable.

As the AgAlCu system lacks the necessary contrast for x-ray investigations, an *in-situ* analysis using XRR is not possible for this alloy system. Therefore, *in-situ* radiography experiments were conducted using the neutron source of the FRMII in Munich. The sample pair Al_{73.6}Cu_{13.8}Ag_{12.6}\Al_{63.6}Cu_{13.8}Ag_{22.6} [at%] was investigated with NR in a suitable *in-situ* LC oven [23]. For the quasi-binary analysis of the diffusion profile, it is required that the contrast changes during the experiment are solely caused by changes in the silver and aluminum concentrations, while the copper concentration remains constant. In particular, there must be no uphill diffusion, i.e. diffusion against the concentration gradient, which is observed in some multi-component systems [50].

For a comprehensive examination of diffusion in the AgAlCu system, the SC method was applied combined with a subsequent chemical analysis per atomic absorption spectroscopy (AAS) [51]. Combining these measurement and analysis methods, sample pairs with little x-ray or neutron contrast can be investigated very accurately in *ex-situ* measurements. For each of the three investigated sample pairs (see table 1), three SC experiments with identical process parameters and subsequent quasi-binary analysis were conducted.

Figure 2 exemplary shows the results of the chemical analysis of Al_{68.6}Cu_{18.8}Ag_{12.6}\ Al_{68.6}Cu_{8.8}Ag_{22.6} [at%] with a subsequent fit of a Gaussian error function [52]. No changes in the aluminum concentration over the entire sample length could be detected after experiment completion proving the assumption that no uphill diffusion of aluminum occurs. The diffusion coefficient was determined as $D_{\rm AgCu}^* = (4.1 \pm 0.4) \cdot 10^{-9} {\rm m}^{-2} {\rm s}^{-1}$ and lies, compared with the other SC experiments, within a 10% error margin. The diffusion coefficients shown in figure 3 are listed in table A2.

Within the error margin of 10%, the thus determined interdiffusion coefficients are equal for the experiments with the same composition as well as in comparison with the other two sample pairs (see figure 3). Further comparison with the diffusion coefficient $D_{\text{AlAg}}^* = (4.4 \pm 0.4) \cdot 10^{-9} \text{m}^{-2} \text{s}^{-1}$ of the system $\text{Al}_{73.6}\text{Cu}_{13.8}\text{Ag}_{12.6} \setminus \text{Al}_{63.6}\text{Cu}_{13.8}\text{Ag}_{22.6}$ [at%] as determined by NR, shows that these are also lie within the expected error margin of 10% (see figure 3). In conclusion, the Ag–Al–Cu sample pair close to its ternary eutectic $\text{Al}_{69.1}\text{Ag}_{18.1}\text{Cu}_{12.8}$ [at%] can be described by a single diffusion coefficient determined by averaging to

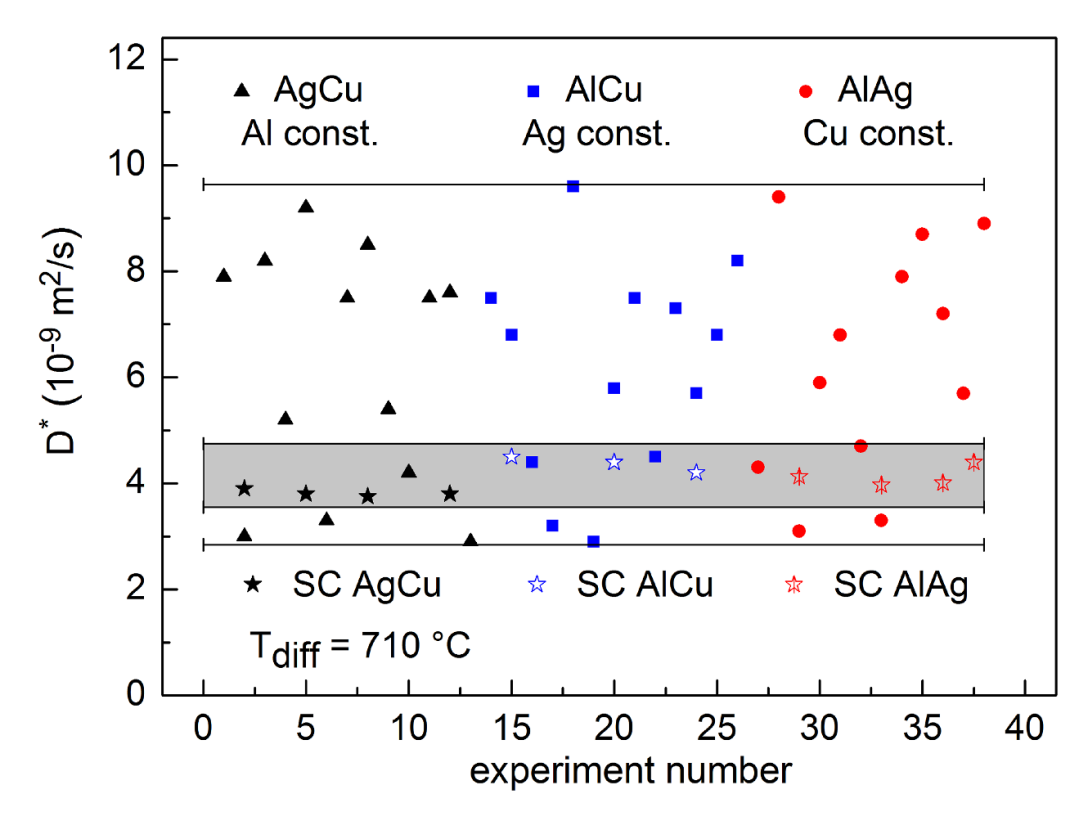


Figure 1. Interdiffusion coefficients of *ex-situ* LC experiments (triangles, squares, circles) with Al–Ag–Cu in comparison with those from shear cell (SC) and *in-situ* neutron radiography experiments (stars). The scattering around the mean value is approximately $\pm 50\%$ for the LC diffusion data and $\pm 10\%$ for the shear cell and *in-situ* data.

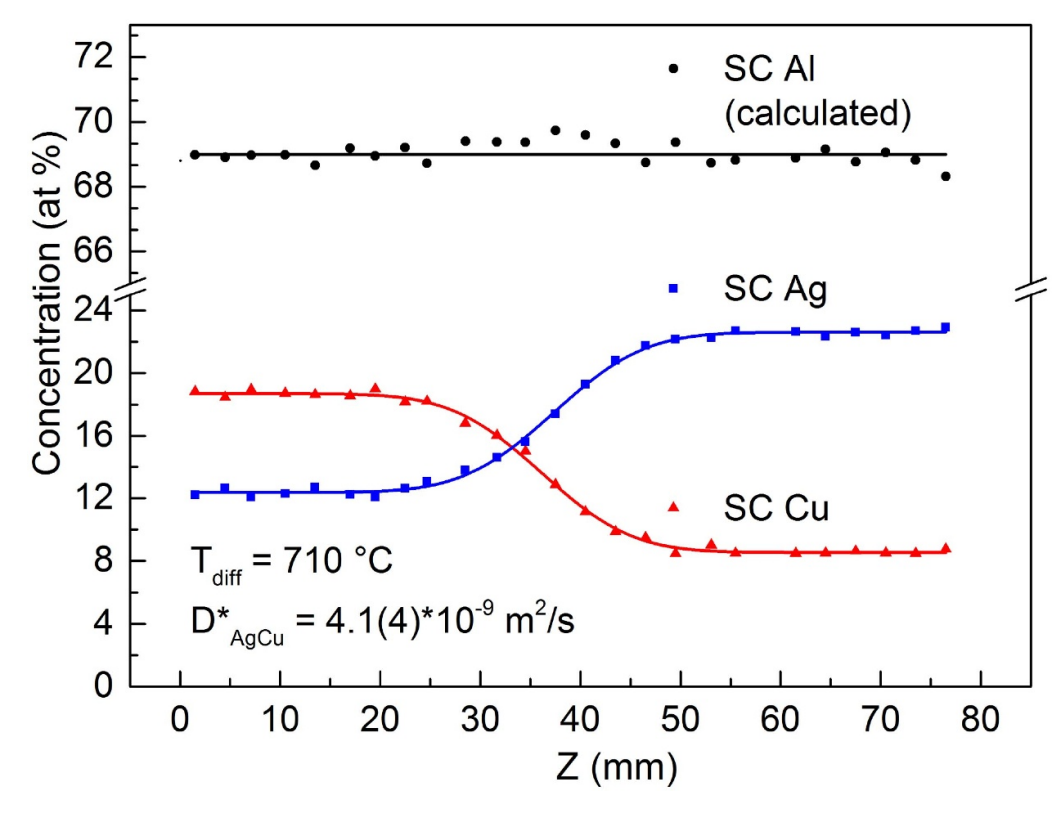


Figure 2. Evaluation of an *ex-situ* shear cell experiment with subsequent AAS analysis using the example of $Al_{68.6}Cu_{18.8}$ $Ag_{12.6} \setminus Al_{68.6}Cu_{8.8}Ag_{22.6}$ [at%]. The concentrations of silver and copper were determined chemically, the one of aluminum was calculated. z indicates the position on the sample along the sample length.

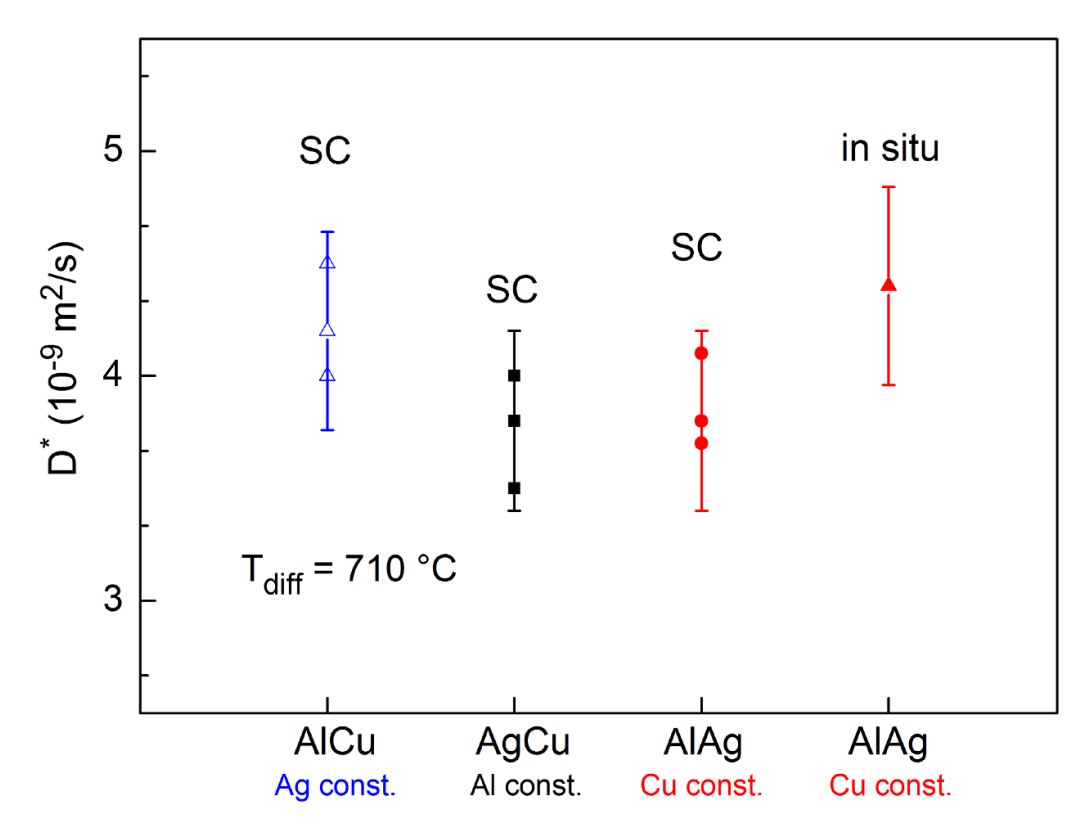


Figure 3. Diffusion coefficients determined by quasi-binary analysis of the shear cell experiments and the inter-diffusion coefficient from the *in-situ* neutron radiography experiment at the FRMII. Within the depicted error margins of 10% around the average of the measurement values, all measured diffusion coefficients are identical.

 $D_{A/B}^* = (4.1 \pm 0.4) \cdot 10^{-9} \text{m}^{-2} \text{s}^{-1}$ within the range of error of 10%

Contrasting the *ex-situ* LC method readings with those from the SC and NR experiments reveals that fewer than 15% of the LC values fall within the margin of error of the other two measurement methods (see figure 1).

3.2. Ternary analysis

To further verify the suitability of the quasi-binary approach described in the preceding section, we conducted a ternary analysis of the Al–Ag–Cu system. In complex ternary systems the applicability of the quasi-binary diffusion analysis to alloys with one constant component cannot be assumed *a priori*. In these systems, uphill diffusion can occur, that is to say, the mass diffusion of one component can be influenced by interactions with the other alloy components, which are caused by their chemical concentration gradients.

During this study, three Al-Ag-Cu sample pairs close to the ternary eutectic Al_{69.1}Ag_{18.1}Cu_{12.8} [at%] [35, 53] and with varying concentrations of all three constituents (see table 2) were investigated with the SC method. The goal is to describe all conducted experiments and their correlative concentration profiles by a single diffusion matrix. In a ternary mixture,

diffusion is characterized by a matrix

$$D = \left(egin{array}{cc} D_{11} & D_{12} \ D_{21} & D_{22} \end{array}
ight).$$

The secondary diagonal elements D_{12} , D_{21} describe the interactions of the components among each other, the main diagonal elements D_{11} , D_{22} the systems' diffusion coefficients. Detailed derivations and information about the theoretical coherences and the physical background can be found in the works of Cooper [54], Anderson [55] and Gupta and Cooper [56].

The quality of the measured data is of essential importance for the unambiguous identification of the total minimum of the correlated Gaussian error functions of all concentration profiles and crucially affects the derivation of the diffusion matrix. It is deduced from the measured concentration profiles by the simultaneously fitting of the interdependent error functions via a Levenberg–Marquard-algorithm under minimization of χ^2 . The choice of the start values for this algorithm and the thereby defined diffusion matrix is essential to avoid accidental convergence of the χ^2 -test in a local minimum as solution for the matrix [57]. Erroneous convergence can also occur if the deviations within the individual concentration profiles within the margins of error are too large and therefore inconsistent.

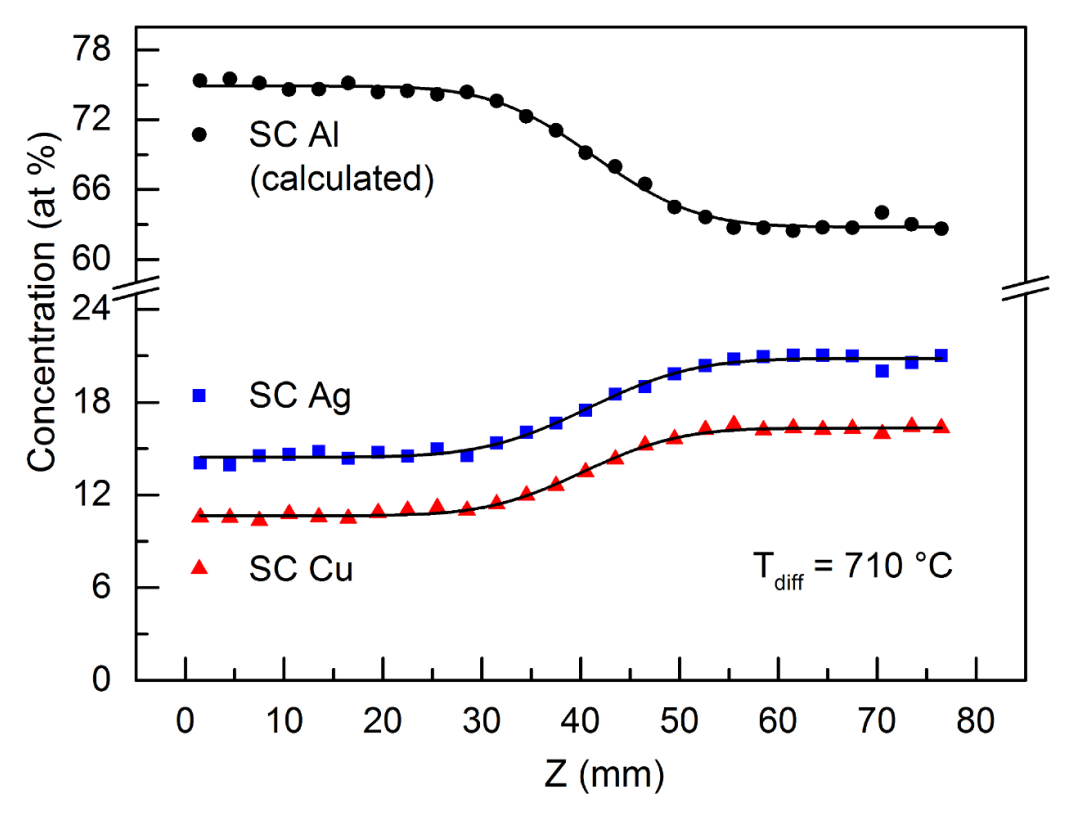


Figure 4. Concentration profiles obtained from a shear cell experiments of the sample $Al_{65.7}Cu_{10.9}Ag_{23.4} \setminus Al_{71.5}Cu_{16.7}Ag_{11.8}$ [at%] as a function of the position along the sample length Z. Silver and copper concentrations were determined by AAS analysis, the aluminum concentration was complemented to 100%.

The experiments conducted on the AgAlCu samples, with the sample composition given in table 2, were used to test the functionality of this analysis method and to verify the in the previous section experimentally proven absence of uphill diffusion also analytically. In these experiments, the concentrations of all components varied between all sample pairs. Identification of the diffusion matrix by determining the total minimum requires several experimental runs with different sample pairs. Therefore, nine sample pairs were used in four experiments. The derived experimental data could be described with deviation of the error function of 20% maximum (see figure 4). The error functions include the interdependency of the three components. The uncertainty in the analysis of a single experiment is a combination of the error in the chemical analysis using AAS and the standard deviation in the error function fit.

The use of the χ^2 -test for the discussed measurements enabled the order of magnitude of the diffusion matrix entries to be determined:

$$D_{\rm AlAgCu} = \left(\begin{array}{cc} 10^{-9} & 10^{-12} \\ 10^{-13} & 10^{-9} \end{array} \right) {\rm m}^{-2} \, {\rm s}^{-1}.$$

The ambiguous convergence discussed, prohibits further specification of the values of the matrix elements. Based on the chosen initial values, the diffusion coefficients fluctuate between $3.5-5\cdot 10^{-9} \mathrm{m}^{-2} \, \mathrm{s}^{-1}$, which lies within the

calculated margin of error for the quasi-binary analysis (see figure 3). Even without the exact values, it is obvious that the secondary diagonal matrix elements are orders of magnitudes smaller than the diffusion coefficients on the main diagonal. This analytically proves the negligible nature of uphill diffusion and justifies the continued application of the quasi-binary approach in the previous chapter.

A recent study of diffusion in liquid $Ce_{70}Al_{10}Cu_{20}$ at 837 K, it was found that the dynamics are dominated by the main diffusion coefficients, with cross diffusion coefficients amounting to only around 10% of the main diffusion coefficients [11]. While this tendency is consistent in both alloys, the cross diffusion coefficients are smaller still in the case of eutectic $Al_{69.1}Ag_{18.1}Cu_{12.8}$ [at%].

This finding makes the simulation of liquid metals and their solidification behavior less complex. As the off-diagonal elements can be neglected and the diagonal elements are similar, a single coefficient would suffice to simulate the diffusion process for this alloy.

3.3. Self-diffusion

The self-diffusion of eutectic Al_{65.7}Cu_{10.9}Ag_{23.4} was determined using QENS. For neutrons, copper has an incoherent scattering cross section of 0.55 barn and for silver the incoherent scattering cross section is very similar with 0.58 barn. In

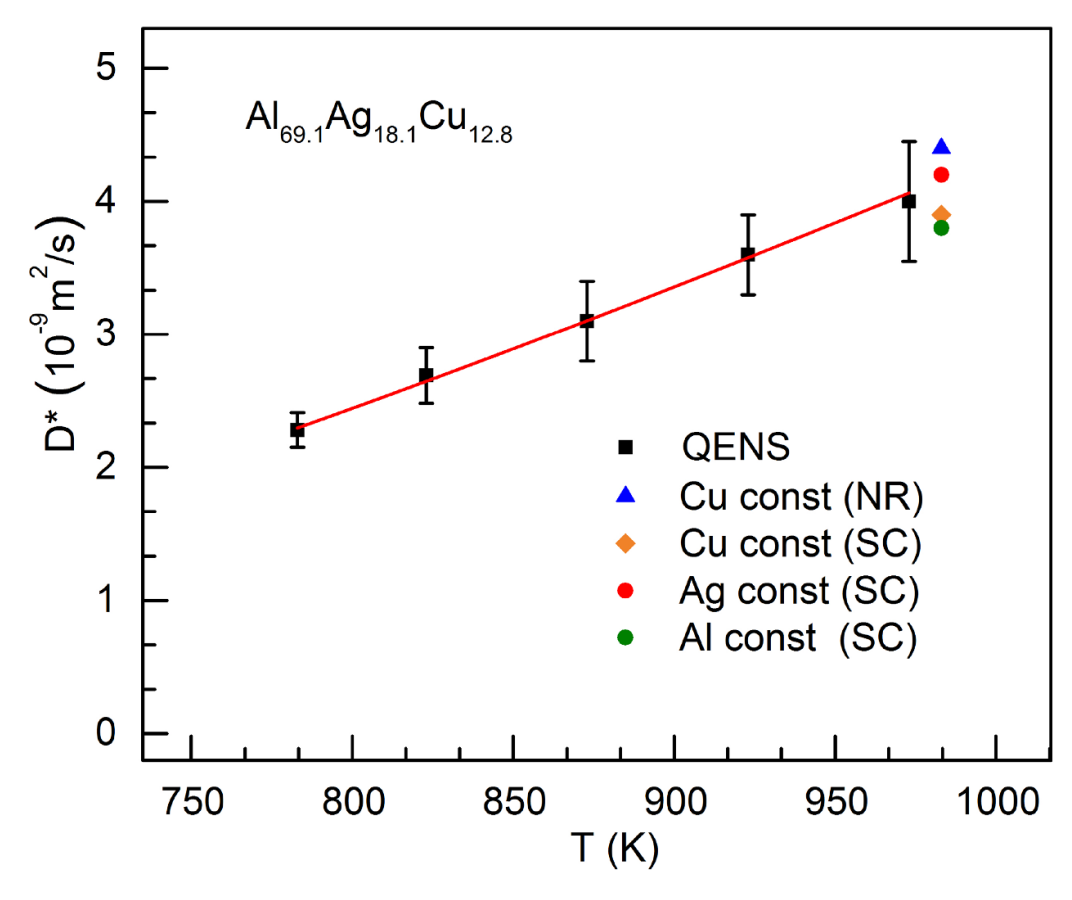


Figure 5. Interdiffusion coefficients measured with neutron radiography (NR) *in-situ* and in a shear-cell (SC) with post-mortem sample analysis and average self-diffusion coefficients by quasielastic neutron scattering (QENS). The solid line represents an Arrhenius fit to the QENS data.

contrast, the incoherent scattering cross section for aluminum is much lower at 0.0082 barn [58].

We assume that the incoherent cross section relate individually to the atomic species and hence the contribution of aluminum can be neglected. The measured data can be described by a single Lorentzian line, so the self-diffusion coefficients of copper and silver can be assumed to be equal to within a factor of two. However, recent publications [59] suggest a different treatment of incoherent cross sections in multicomponent systems which is still debated. In this case, the aluminum contribution would not be negligible. However, the experiment results of the single Lorentzian line would suggest equal self-diffusion for all three elements within a factor of two.

The result of the QENS measurements at different temperatures is shown in figure 5. The red line is a fit with the Arrhenius function

$$D = D_0 \exp\left(\frac{-Q}{k_{\rm B}T}\right)$$

where Q is the activation energy, $k_{\rm B}$ Boltzmann constant and T the absolute temperature. The fit yields the parameters $D_0 = (41 \pm 3) \mathrm{x} 10^{-9} \, \mathrm{m}^{-2} \, \mathrm{s}^{-1}$ and $Q = 194 \, \mathrm{meV}$. The activation energy is therefore very similar to the binary $\mathrm{Al}_{80}\mathrm{Ag}_{80}$

with $176 \pm 6 \text{ meV} [60]$ but lower than for pure silver with 288 $\pm 10 \text{ meV} [60]$.

Interdiffusion data (as in figure 3) are also depicted for comparison. As can be seen, the interdiffusion and self-diffusion coefficients agree within error bars. This indicates that kinetic contributions to interdiffusion are significant in this ternary melt.

4. Conclusion

The liquid Al-Ag-Cu system around its ternary eutectic Al_{69.1}Ag_{18.1}Cu_{12.8} [at%] was studied systematically, and its diffusion coefficients were measured. A combination of different techniques was applied in this study and revealed that traditional LC experiments are considerably less reliable than *in-situ* and SC experiments.

When analyzing diffusion in complex ternary alloy systems with one constant constituent, it cannot be assumed *a priori* that the quasi-binary approach is applicable. In such systems, the mass diffusion of one component may be influenced by interactions with other alloy constituents due to their chemical concentration gradients. For the investigated sample pairs with one constant component concentration, it was shown both experimentally and analytically, using a diffusion matrix, that

no uphill diffusion occurs and that the quasi-binary ansatz can be used. The such derived diffusion coefficients for the SC and NR experiments coincide within their margins of error of 10%. Hence a single diffusion coefficient is sufficient for the continuing modeling approach to the examined system.

Using QENS, the temperature dependence of the self-diffusion coefficient was obtained. It was found that interdiffusion and self-diffusion agree within errorbars, proving the predominance of the mass transport over the thermodynamic driving forces in the diffusion processes investigated.

As Al-Ag-Cu is one of the rare alloys for which ternary diffusion has been measured in the liquid, these results will be used for further simulations of ternary liquid alloys, as well as for experimental studies of e.g. thermodiffusion in molten Al-Ag-Cu.

Data availability statement

The data cannot be made publicly available upon publication because the cost of preparing, depositing and hosting the data would be prohibitive within the terms of this research project. The data that support the findings of this study are available upon reasonable request from the authors.

Acknowledgments

We thank Sebastian Stüber and Tobias Unruh for their support during the quasielastic neutron scattering measurement and the Forschungsneutronenquelle Heinz Maier-Leibnitz for the beamtime on ToF-ToF. We thank Benjamin Ignatzi and Matthias Kolbe for support in sample analysis.

Appendix

Table A1. Diffusion coefficients in 10^{-9} m² s⁻¹ as obtained by *ex-situ* LC measurements (LC). For the measurements a quasi-binary approach is used where the composition of the elements mentioned in the column heading are varied while the third component is kept constant.

AlCu LC	AgCu LC	AgAl LC
7.5	7.9	4.3
6.8	3.0	9.4
4.4	8.2	3.1
3.2	5.2	5.9
9.6	9.2	6.8
2.9	3.3	4.7
5.8	7.5	3.3
7.5	8.5	7.9
4.5	5.4	8.7
7.3	4.2	7.2
5.7	7.5	5.7
6.8	7.6	8.9
8.2	2.9	

Table A2. Diffusion coefficients in 10^{-9} m² s⁻¹ as obtained by shear cell measurements (SC) and by neutron radiography (*in situ*). The uncertainty of these values is 10%. For the measurements a quasi-binary approach is used where the composition of the elements mentioned in the column heading are varied while the third component is kept constant.

AlCu So	C AgCu SC	AgAl SC	AgAl in-situ
4.5	4.0	4.1	4.4
4.2	3.8	3.7	
4.0	3.5	3.8	
	3.8		

ORCID iDs

F Kargl © 0000-0001-9902-0420 E Sondermann © 0000-0001-5935-8945 A Meyer © 0000-0002-0604-5467

References

- [1] Boettinger W J, Coriell S R, Greer A L, Karma A, Kurz W, Rappaz M and Trivedi R 2000 Solidification microstructures: recent developments, future directions Acta Mater. 48 43–70
- [2] Zhang L, Du Y, Steinbach I, Chen Q and Huang B 2010 Diffusivities of an Al-Fe-Ni melt and their effects on the microstructure during solidification *Acta Mater*. 58 3664-75
- [3] Pablo H, Schuller S, Toplis M J, Mostefaoui S, Mesbah A and Roskosz M 2019 Impact of chemical diffusion on crystal growth in sodium borosilicate glasses J. Non-Cryst. Solids 503–504 313–22
- [4] Klein T, Kankanamge C J, Koller T M, Rausch M H, Fröba A P, Assael M J, Wakeham W A, Guevara-Carrion G and Vrabec J 2025 Definitions and preferred symbols for mass diffusion coefficients in multicomponent fluid mixtures including electrolytes (iupac technical report) Pure Appl. Chem. 97 689–713
- [5] Miller D G, Vitagliano V and Sartorio R 1986 Some comments on multicomponent diffusion: negative main term diffusion coefficients, second law constraints, solvent choices and reference frame transformations J. Phys. Chem. 90 1509–19
- [6] Jiayin Li, Wang J, Xinxin Li and Qin J 2024 Composition-dependent diffusion and viscosity behavior in liquid Ti–Al–Ni ternary alloys *J. Mater. Res. Technol.* 33 3864–73
- [7] Legros J C, Gaponenko Y, Mialdun A, Triller T, Hammon A, Bauer C, Köhler W and Shevtsova V 2015 Investigation of Fickian diffusion in the ternary mixtures of water-ethanol-triethylene glycol and its binary pairs *Phys. Chem. Chem. Phys.* 17 27713–25
- [8] Changfa D, Zheng Z, Min Q, Yong D, Liu Y, Deng P, Zhang J, Wen S and Liu D 2020 A novel approach to calculate diffusion matrix in ternary systems: application to Ag–Mg–Mn and Cu–Ni–Sn systems Calphad 68 101708
- [9] Jaques A V and LaCombe J C 2007 Assessment of ternary multicomponent diffusion in alloy 22 (Ni-Cr-Mo) *Defect Diffus. Forum* 266 181–90
- [10] Zhou Z, Cui Y, Qiaojun W, Guanglong X, Zhou L and Cui Y 2022 Experimental diffusion research and assessment of diffusional mobility in HCP Mg–Al–Ga ternary alloys Calphad 78 102437

- [11] Hu J L, Zhong L X, Chen C, Li D D and Zhang B 2021 A new analysis method based on the onsager reciprocal relations for interdiffusion in a multicomponent melt *J. Appl. Phys.* 129 125101
- [12] Wang R, Chen W, Tang Y, Zhang L, Yong D, Jin Z and Živković D 2016 Diffusivities, atomic mobilities and simulation of ternary eutectic solidification in the Ag–Al–Cu melts J. Mater. Sci. 51 5979–91
- [13] Wang R, Chen W, Zhang L, Liu D, Li Xi, Yong D and Jin Z 2013 Diffusivities and atomic mobilities in the Al–Ce–Ni melts J. Non-Cryst. Solids 379 201–7
- [14] Zhong W and Zhao J-C 2022 Recommendations for simplified yet robust assessments of atomic mobilities and diffusion coefficients of ternary and multicomponent solid solutions Scr. Mater. 207 114227
- [15] Banish R M and Jalbert L B 1999 In-situ diffusivity measurement technique Adv. Space Res. 24 1311–20
- [16] Griesche A, Macht M-P, Garandet J-P and Frohberg G 2004 Diffusion and viscosity in molten Pd₄₀Ni₄₀P₂₀ and Pd₄₀Cu₃₀Ni₁₀P₂₀ alloys J. Non-Cryst. Solids 336 173–8
- [17] Shimoji M and Itami T 1986 Atomic Transport in Liquid Metals (Trans-Tech Publications, Brookfield)
- [18] Meyer A, Hennig L, Kargl F and Unruh T 2019 Iron self diffusion in liquid pure iron and iron-carbon alloys J. Phys.: Condens. Matter 31 395401
- [19] Yang L, Simnad M T and Derge G 1956 Self-diffusion of iron in molten Fe-C alloys J. Metals 8 1577–80
- [20] Botton V, Lehmann P, Bolcato R, Moreau R and Haettel R 2001 Measurement of solute diffusivities. Part II. Experimental measurements in a convection-controlled shear cell. interest of a uniform magnetic field *Int. J. Heat* Mass Transfer 44 3345–57
- [21] Meyer A and Kargl F 2013 Diffusion of mass in liquid metals and alloys-recent experimental developments and new perspectives *Int. J. Microgravity Sci. Appl.* 30 30–35
- [22] Griesche A, Zhang B, Solórzano É and Garcia-Moreno F 2010 Note: x-ray radiography for measuring chemical diffusion in metallic melts Rev. Sci. Instrum. 81 056104
- [23] Kargl F, Engelhardt M, Yang F, Weis H, Schmakat P, Schillinger B, Griesche A and Meyer A 2011 In situ studies of mass transport in liquid alloys by means of neutron radiography J. Phys.: Condens. Matter 23 254201
- [24] Petit J and Norman H N 1956 Self-diffusion in liquid gallium J. Chem. Phys. 24 1027–8
- [25] Heuskin D, Kargl F, Griesche A, Ch Stenzel D M, Bräuer D and Meyer A 2011 MSL compatible isothermal furnace insert for high temperature shear-cell diffusion experiments J. Phys.: Conf. Ser. 327 012053
- [26] Horbach J, Das S K, Griesche A, Macht M-P, Frohberg G and Meyer A 2007 Self-diffusion and interdiffusion in Al₈₀Ni₂₀ melts: Simulation and experiment *Phys. Rev. B* 75 174304
- [27] Sondermann E, Kargl F and Meyer A 2016 Influence of cross correlations on interdiffusion in Al-rich Al-Ni melts *Phys. Rev. B* 93 184201
- [28] Yang F, Heintzmann P, Kargl F, Binder K, Nowak B, Schillinger B, Voigtmann T and Meyer A 2018 Kinetics-dominated interdiffusion in metallic glass-forming liquids *Phys. Rev. B* 98 064202
- [29] Hu J L, Zhong L X, Zhu C A and Zhang B 2017 Inter-diffusion and its correlation with dynamical cross correlation in liquid Ce80Ni20 Appl. Phys. A 123 176
- [30] Belova I V, Heuskin D, Sondermann E, Ignatzi B, Kargl F, Murch G E and Meyer A 2018 Combined interdiffusion and self-diffusion analysis in Al-Cu liquid diffusion couple Scripta Mater. 43 40
- [31] Kuhn P, Horbach J, Kargl F, Meyer A and Voigtmann T 2014 Diffusion and interdiffusion in binary metallic melts *Phys. Rev. B* 90 024309

- [32] Darken L S 1948 Diffusion, mobility and their interrelation through free energy in binary metallic systems *Trans. AIME* 175 184–201
- [33] Liu X, Schnell S K, Simon J-M, Krüger P, Bedeaux D, Kjelstrup S, Bardow A and Vlugt T J H 2013 Diffusion coefficients from molecular dynamics simulations in binary and ternary mixtures *Int. J. Thermophys.* 34 1169
- [34] White A J, Ticknor C, Meyer E R, Kress J D and Collins L A 2019 Multicomponent mutual diffusion in the warm, dense matter regime *Phys. Rev. E* 100 033213
- [35] Witusiewicz V T, Hecht U, Fries S G and Rex S 2005 The Ag–Al–Cu system: II. A thermodynamic evaluation of the ternary system J. Alloy Compd. 387 217–27
- [36] Müller H and Müller-Vogt G 2003 Investigation of additional convective transports in liquid metals and semiconductors during diffusion measurements by means of the shear cell technique Cryst. Res. Technol. 38 707–15
- [37] Roşu-Pflumm R, Wendl W, Müller-Vogt G, Suzuki S, Kraatz K-H and Frohberg G 2009 Diffusion measurements using the shear cell technique: investigation of the role of Marangoni convection by pre-flight experiments on the ground and during the Foton M2 mission *Int. J. Heat Mass Transfer* **52** 6042–9
- [38] Ruiz X, Sáez N, Gavaldà J and Pallarès J 2015 On the impact of free surfaces on the measurement of diffusion coefficients in metallic binary alloys using shear cells *Int. J. Heat Mass Transfer* 81 602–17
- [39] Dennstedt A, Helfen L, Steinmetz P, Nestler B and Ratke L 2015 3D synchrotron imaging of a directionally solidified ternary eutectic *Met. Mater. Trans. A* 47 981–4
- [40] Dennstedt A and Ratke L 2012 Microstructures of directionally solidified Al–Ag–Cu ternary eutectics *Trans. Indian Inst. Met.* 65 777–82
- [41] Garandet J P, Barat C and Duffar T 1995 The effect of natural convection in mass transport measurements in dilute liquid alloys Int. J. Heat Mass Transfer 38 2169–74
- [42] Kargl F, Sondermann E, Weis H and Meyer A 2013 Impact of convective flow on long-capillary chemical diffusion studies of liquid binary alloys *High Temp. High Press.* 42 3–21
- [43] Griesche A, Garcia Moreno F, Macht M-P and Frohberg G 2006 Chemical diffusion experiments in AlNiCe-melts Materials Science Forum vol 508 (Trans. Tech. Publ.) pp 567–72
- [44] Zhang B, Griesche A and Meyer A 2010 Diffusion in Al-Cu melts studied by time-resolved x-ray radiography *Phys. Rev. Lett.* 104 035902
- [45] Suzuki S, Kraatz K-H, Griesche A and Frohberg G 2005 Shear cell development for diffusion experiments in FOTON-satellite missions and on the ground with consideration of shear-induced convection *Microgravity-Sci. Technol.* 16 127–32
- [46] Meyer A, Stüber S, Holland-Moritz D, Heinen O and Unruh T 2008 Determination of self-diffusion coefficients by quasielastic neutron scattering measurements of levitated Ni droplets *Phys. Rev. B* 77 092201
- [47] Meyer A 2015 The measurement of self-diffusion coefficients in liquid metals with quasielastic neutron scattering EPJ Web of Conferences vol 83 p 01002
- [48] Unruh T, Neuhaus J and Petry W 2007 The high-resolution time-of-flight spectrometer TOFTOF Nucl. Inst. Methods Phys. Res. Sec. A 580 1414–22
- [49] Sadhu S, Chakraborty A, Makineni S, Bhattacharyya S and Paul A 2024 An experimental estimation method of diffusion coefficients in ternary and multicomponent systems from a single diffusion profile *Acta Mater*. 274 120000
- [50] Griesche A, Macht M-P and Frohberg G 2005 Chemical diffusion in bulk glass-forming Pd40Cu30Ni10P20 melts Scr. Mater. 53 1395–400

- [51] Baker D E and Suhr N H 1982 Atomic absorption and flame emission spectrometry *Methods of Soil Analysis: Part 2* Chemical and Microbiological Properties pp 13–27
- [52] Cussler E L 2009 Diffusion: Mass Transfer in Fluid Systems (Cambridge University Press)
- [53] Witusiewicz V T, Hecht U, Fries S G and Rex S 2004 The Ag–Al–Cu system: Part I: reassessment of the constituent binaries on the basis of new experimental data *J. Alloys* Compd. 385 133–43
- [54] Cooper A R 1968 The use and limitations of the concept of an effective binary diffusion coefficient for multicomponent diffusion *Mass Transport in Oxides* vol 296 pp 79–84
- [55] Anderson D E 1981 Chapter 6. Diffusion in electrolyte mixtures *Kinetics of Geochemical Processes* vol 8 (De Gruyter) pp 211–60

- [56] Gupta P K and Cooper A R 1971 The [D] matrix for multicomponent diffusion *Physica* **54** 39–59
- [57] Trial A F and Spera F J 1994 Measuring the multicomponent diffusion matrix: Experimental design and data analysis for silicate melts *Geochim. Cosmochim. Acta* 58 3769–83
- [58] Sears V F 1992 Neutron scattering lengths and cross sections Neutron News 3 26–37
- [59] Shahzad A et al 2024 Atomic diffusion in liquid gallium and gallium-nickel alloys probed by quasielastic neutron scattering and molecular dynamic simulations J. Phys.: Condens. Matter 36 175403
- [60] Engelhardt M, Meyer A, Yang F, Simeoni G G and Kargl F 2016 Self and chemical diffusion in liquid Al-Ag Defect Diffus. Forum 367 157–66